APPLICATE

H2020 - Research and Innovation Action

Advanced Prediction in Polar regions and beyond: Modelling, observing system design and LInkages associated with a Changing Arctic climaTE

Grant Agreement No: 727862

Deliverable No. 3.2

Report on coordinated atmosphere-only multi-model assessment of the seasonal to inter-annual impact of Arctic sea ice decline on lower latitudes

Submission of Deliverable

Work Package	WP3 Atmosperic and oceanic linkages
Deliverable No	3.2
Deliverable title	Report on coordinated atmosphere-only multi-model assessment of the seasonal to inter-annual impact of Arctic sea ice decline on lower latitudes
Version	
Status	Final
Dissemination level	PU - Public
Lead Beneficiary	6 - MET Norway
Contributors	☒ 1 – AWI ☒ 2 – BSC ☐ 3 - ECMWF ☐ 4 – UiB ☐ 5 – UNI Research ☒ 6 – MET Norway ☒ 7 – Met Office ☐ 8 – UCL ☐ 9 - UREAD ☐ 10 – SU ☐ 11 – CNRS-GAME ☒ 12 - CERFACS ☐ 13 – AP ☐ 14 – UiT ☐ 15 - IORAS ☐ 16 - MGO
Due Date	31 October 2019
Delivery Date	31 October 2019
Coordinating author	Lise Seland Graff (lise.s.graff@met.no)
Contributing authors	Rosie Eade and Doug Smith (Met Office), Xavier J. Levine, Ivana Cvijanovic, Markus Donat, Pablo Ortega (BSC-CNS), Rym Msadek, Laurent Terray, Svenya Chripko, Emilia Sanchez (CERFACS), and Tido Semmler (AWI).

This project has received funding from the European Union's Horizon 2020 Research & Innovation programme under grant agreement No. 727862.

Table of Contents

EXECUTIVE SUMMARY

Work package 3 within APPLICATE examines atmospheric and oceanic linkages with the objectives of (1) advancing our understanding of the mechanisms by which the mid-latitude weather and climate could respond to the substantial Arctic climate change that is expected in the coming decades and (2) coordinate a suite of novel multi-model experiments designed to identify the oceanic and atmospheric linkages between the Arctic region and the northern mid-latitudes. Deliverable 3.2 presents results from two of these experiments in which the impact of Arctic sea-ice loss is investigated using state-of-the-art climate models forced by sea-ice concentrations from the present-day climate and from a climate with reduced sea-ice concentrations in the Arctic. Investigating the difference between these model experiments allows us to assess the effect of Arctic sea-ice decline, focusing on lower latitudes. This is relevant for the project objectives of APPLICATE, which is to *develop enhanced predictive capacity for weather and climate in the Arctic and beyond, and to determine the influence of Arctic climate change on Northern Hemisphere mid-latitudes, for the benefit of policy makers, businesses and society*.

Results show that Arctic sea-ice loss is associated with significant low-level warming over the Arctic region. The warming is strongest during boreal autumn and winter. In these seasons, the near-surface temperature response is largest in the regions where the sea ice is changing the most, over the Arctic Basin during autumn and more over the marginal seas during winter; but temperature changes are also occurring in regions in Eastern Europe, Siberia, and North America. Most models show an equatorward shift of the Northern Hemisphere tropospheric jet stream during winter, but there is large variation in the magnitude of the response. Furthermore, even the sign of the response of the stratospheric jet is uncertain. We find a significant low-pressure anomaly residing over the central Arctic during fall. During winter, the response varies more from model to model, but there is generally an increase in pressure in the Icelandic region and decrease further south (though the significance varies between models), in line with a negative phase of the NAO and an equatorward shift of the tropospheric jet.

A shift in the tropospheric jet has potential ramifications for extreme events. We find a significant decrease in surface winds and precipitation during winter over Northern Europe in HadGEM3-GA7.1, which corroborates results from the recent APPLICATE case study 1 which highlights the potential role of low autumn Arctic sea ice leading to extreme climate events at mid-latitudes the following winter. Extreme weather and Arctic amplification has also been linked to changes in the waviness of the atmospheric flow. We find a significant influence of Arctic sea-ice loss on planetary-scale waves during summer in CNRM-CM6. However, no significant differences are found during winter, nor for synoptic-scale waves for either season. These results are corroborated by results from ECHAM6.3, using a sinuosity index.

The spread in model responses reported here is expected and desirable since it potentially allows the real-world situation to be diagnosed using the "emergent constraint" framework. A key part of this will be to understand the physical processes in detail and hence develop an observable metric to explain the differences between models and reduce the uncertainty. Other experiments within APPLICATE are aimed at understanding the physical processes, specifically using coupled models and testing the sensitivity to regional sea-ice changes and model biases. These will be reported in future deliverables D3.1 and D3.3. An important achievement of APPLICATE has been establishing the Polar Amplification Model Intercomparison Project (PAMIP), which includes the experiments described above and expands the set of models beyond those run by the APPLICATE partners. An overall synthesis of results from APPLICATE and PAMIP will be presented in D3.4.

1. INTRODUCTION

1.1. Background and objectives

The aim of APPLICATE is to *develop enhanced predictive capacity for weather and climate in the Arctic and beyond, and to determine the influence of Arctic climate change on Northern Hemisphere mid-latitudes, for the benefit of policy makers, businesses and society*.

Work package 3 within APPLICATE examines atmospheric and oceanic linkages with the objectives of (1) advancing our understanding of the mechanisms by which the mid-latitude weather and climate could respond to the substantial Arctic climate change that is expected in the coming decades and (2) coordinate a suite of novel multi-model experiments designed to identify the oceanic and atmospheric linkages between the Arctic region and the northern mid-latitudes. Deliverable 3.2 focuses on a sub-set of these experiments in which Arctic sea-ice decline is investigated using state-of-the-art climate models forced with present-day values for sea surface temperatures (SSTs) and values for sea ice concentrations (SIC) corresponding to (1) a future Arctic which is warmer and has less sea ice and (2) the present-day Arctic. Investigating the difference between these model experiments allows us to assess the effect of Arctic sea-ice decline, focusing on lower latitudes.

1.2. Organisation of this report

In what follows we give an overview of the experiments and the models we have used in Section 2. We consider results from four essential climate variables in Section 3: zonal-mean temperature and near-surface temperature (Section 3.1), zonal-mean wind (Section 3.2), and sea-level pressure (Section 3.3). We then consider implications for changes in extreme events under Arctic sea-ice loss (Section 3.4). Conclusions and outlook is given in Section 4.

2. METHODOLOGY

To investigate the impact of Arctic sea-ice loss on the atmospheric circulation, we have designed and performed coordinated multi-model experiments in which the sea ice in the Arctic is prescribed to two different states. In the *present-day experiment*, the sea ice is prescribed to present-day conditions (taken to be the year 2000). In the *future-Arctic experiment*, the sea ice is prescribed to conditions corresponding a climate that is 2 °C warmer than the pre-industrial climate. The SSTs are identical in the two experiments, and are prescribed to present-day conditions.

We employ a set of state-of-the-art climate models (Table 1) in which the atmosphere and land models are active, but the ocean and sea-ice models are replaced by prescribed values. The experiments are 14 months long, starting April 1st 2000 and ending May 31st 2001, and results from the last 12 months are shown here. The models have all produced a large set of ensemble members (100 or more) for each of the two experiments to identify robust responses beyond the natural climate variability. The members are generated by bit-level perturbations to the initial conditions for most models, and by different seeds to the stochastic physics scheme in the Met Office model.

Table 1: overview of climate models contributing to APPLICATE work package 3. Note ECHAM6.3 and OpenIFS are listed in the same column as the results from these two models are averaged together yielding a 400-member ensemble for each experiment (two models run with two different resolutions with 100 members for each model and resolution).

Model	ECHAM6.3 OpenIFS	EC-Earth 3.3	CNRM-CM6	NorESM2-LM	HadGEM3-GA7.1
Partner	AWI	BSC	CERFACS	MET Norway	Met Office
Atmosphere	ECHAM6.3 (T63 & T127) OpenIFS (T159 & T511)	IFS T255 (100 km) L91	ARPEGE-Climat T217 (140 km) L91	CAM-OSLO 2º ×2º L32	MetUM N216 L85
Ensemble size per experiment	400 (100 for each model and resolution)	150	200	100	150
PAMIP	Yes	Yes	Yes	Yes	Yes

An important achievement of APPLICATE has been to develop the Polar Amplification Model Intercomparison Project (PAMIP; Smith et al., 2019) under the sixth Coupled Model Intercomparison Project (CMIP6; Eyring et al, 2016). PAMIP includes the two experiments described above, and thus expands the range of models to the wider international community in order to obtain more robust results. There are currently 14 different models that have completed the two PAMIP simulations that we consider in the present report. While we focus on results from the APPLICATE partners (Table 1), we will also consider some initial results from the full set of currently available PAMIP runs in Section 3.2.

3. RESULTS AND DISCUSSION

In what follows we first consider the response of the full set of models in Table 1 for four essential climate variables: near-surface temperature, zonal-mean temperature, zonal-mean zonal wind, and sea-level pressure. To improve the readability of the text, we only include selected figures in the main text, but the full set of figures from all models is included in Annex 7.1 and are referred to when relevant. In the last subsection, we consider implications for changes in extreme events for a subset of the models.

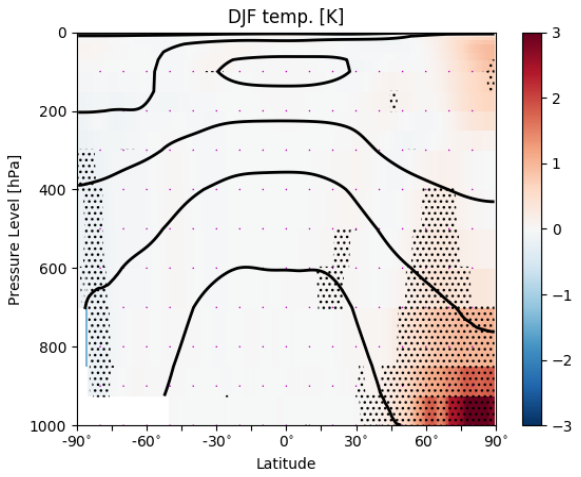

Figure 1: Ensemble-mean change in zonal-mean temperature between the future-Arctic experiment and the present-day experiment (colours) shown with the present-day climatology (solid black lines; intervals of 10 K) from EC-Earth. The fields are shown for winter, defined as the three-month period December–February (DJF). Stippling indicates that the changes are significant at the 95% confidence level. The significance is assessed by computing 1000 samples of ensemble-mean anomalies by randomly bootstrapping members of the present-day and future-Arctic experiments, and requiring for the ensemble-mean anomalies to have the same sign in at least 95% of the bootstrapped samples. Units are K.

3.1 Near-surface temperature

Sea-ice loss in the Arctic is associated with a local thermodynamic response with significant low-level warming in the Arctic region (Figure 1 and Figures 13, 17, 21, 25, and 27 in annex 7.1). There is Arctic amplification of the warming signal during all seasons (albeit rather weak during spring and summer) with the warming being mostly

confined below 600 hPa in all models and with the maximum warming occurring near the surface close to the regions of sea-ice loss (e.g. Screen et al., 2018). The warming is strongest during autumn and winter.

During autumn, the sea-ice reduction primarily occurs over the Arctic basin and this is also where we are seeing the strongest changes in the near-surface temperature (Figure 2 and Figures 11, 15, 19, 23, and 27 in annex 7.1). During winter, the changes are more concentrated over the marginal seas (Karents/Bara, Labrador, and Bering/Okhotsk).

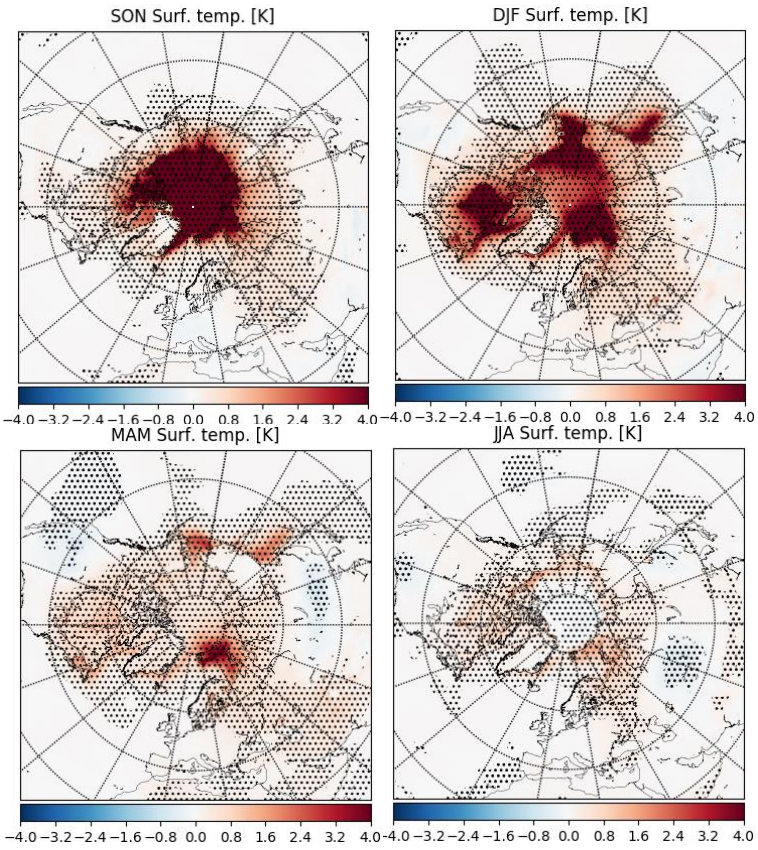

Figure 2: Ensemble-mean change in near-surface temperature between the future warming experiment and the present-day experiment (colours) from EC-Earth. Fields are shown for autumn, defined as the three-month period September–October (SON; upper left), winter (DJF; upper right), spring, defined as March–May (MAM; bottom left), and summer, defined as June–August (JJA; bottom right). Stippling is as in Figure 1. Units are K.

The changes we are seeing during autumn and winter are consistent with the cold atmosphere being warmed by the ocean as the sea-ice cover is reduced. During autumn, an intense warming of the lower troposphere over the Arctic Ocean is expected as the central Arctic is nearly ice-free with warm surface ocean temperatures. As sea ice grows over the central Arctic during winter, only the marginal seas become exposed to the cold overlying atmosphere. The near-surface temperature anomalies then peak more over the marginal seas and not so much over the central Arctic where sea ice isolates the cold atmosphere from the ocean. During spring and summer the temperature differences between the ocean and atmosphere become weaker, consistent with the weak near-surface temperature anomalies.

Over land, warm anomalies are found primarily in areas immediately adjacent to the Arctic basin. Nonetheless, some mid-latitude regions are also found to have significant changes, including regions in Eastern Europe, Siberia, and North America (consistent with Peings et al., 2014). The extent and magnitude of the warming however seems to be model dependent. The models presented here do not show robust and significant cooling over Eurasia in contrast to Honda et al. (2009) and Mori et al. (2014, 2019).

3.2 The zonal-mean wind

The Northern Hemisphere tropospheric winter jet stream weakens on the poleward side in all models and has a relatively weaker strengthening on the equatorward side, consistent with an equatorward shift (Figure 3 below and Figures 14, 18, 22, 26, and 27 in annex 7.1) and in line with some previous studies (e.g. Peings et al., 2014; Deser et al., 2015; Oudar et al., 2017; Blackport and Kushner, 2016, 2017). At present the underlying mechanism is not fully

understood. A weakening of the zonal wind at low altitudes might be expected in response to the reduced the Equator-to-pole temperature gradient. However, the strengthening of the subtropical jet is likely driven by changes in wave activity. Further work within APPLICATE will aim to elucidate the physical mechanism, and understand the causes of model differences.

The tropospheric changes in zonal wind are generally strongest in autumn and winter, consistent with these seasons having the most pronounced changes in temperature. Changes are weaker, and generally not significant, during spring and summer.

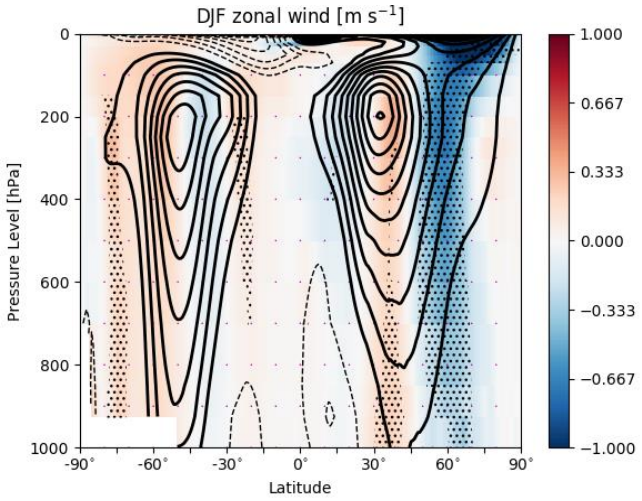

Figure 3: Ensemble-mean change in zonal-mean zonal wind between the future-Arctic experiment and the present-day experiment (colours) during winter (DJF) shown with the present-day climatology (solid black lines; intervals of 4 m s^{-1}) from EC-Earth. Stippling is as in Figure 1. Units are m s^{-1}.

To assess the robustness of the equatorward shift of the Northern Hemisphere tropospheric jet, we consider the response of the 14 different models that have currently completed the PAMIP simulations to assess the response to future-Arctic sea-ice loss (Figure 4).

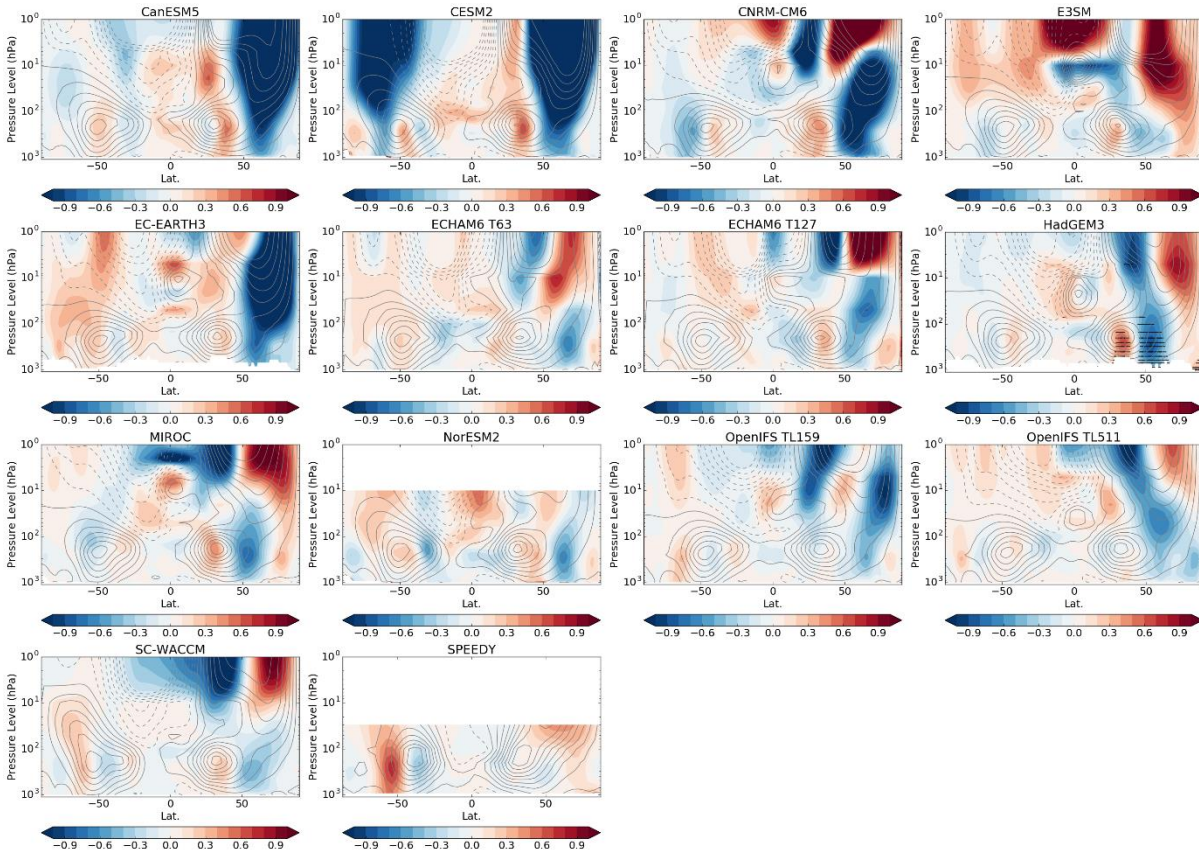

Figure 4: Ensemble-mean change in zonal-mean zonal wind between the future-Arctic and the present-day experiments during winter (DJF) for 14 different models from the international community involved in PAMIP (including the models in Table 1). Grey contour lines show the present-day climatology at 5 m s^{-1} intervals, with dashed lines representing negative values. Units are m s^{-1}.

The majority of models show an equatorward shift of the tropospheric jet in the Northern Hemisphere, consistent with the subset of models we focus on in this report. As expected there is much variation in the strength of the response (Figures 4 and 5). In the stratosphere, there is substantial inter-model variability in both the sign and the strength of the response.

In the CNRM-CM6, the stratospheric jet response is moreover shown to exhibit considerable seasonal variability (Figure 6). The stratospheric jet weakens as the polar vortex weakens following the maximum near-surface warming in November, and this weakening still persists in January. In February, the stratospheric winds flip sign, and the polar vortex is strengthened. Such behavior complicates the interpretation of seasonal means, and moreover the comparison between models, as averaging over several months can partly mask the stratospheric response.

Note it can be beneficial to increase the ensemble size beyond 100 members to attain significant results in the stratosphere, because the internal variability is large compared to the climate change signal caused by Arctic sea-ice loss simulated by the models. We note that the signal-to-

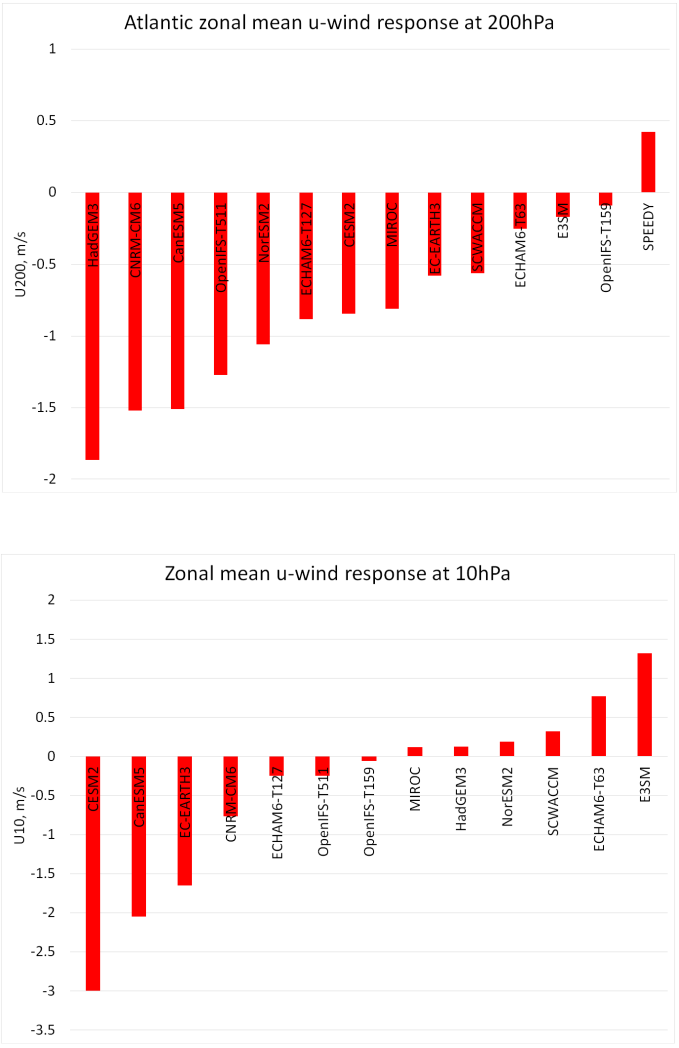

Figure 5: Ensemble-mean change in zonal-mean zonal wind at 200 hPa (top) and at 10 hPa (bottom) between the future-Arctic and the present-day experiments during winter (DJF) for the 14 PAMIP models (Figure 4). Note SPEEDY is not included in the bottom panel because 10 hPa is above the model top. The zonal mean is taken over the Atlantic region for latitudes between 50°N and 60°N in top left panel, and for all longitudes and latitudes between 55°N and 65°N in the bottom panel. Units are m s^{-1}.

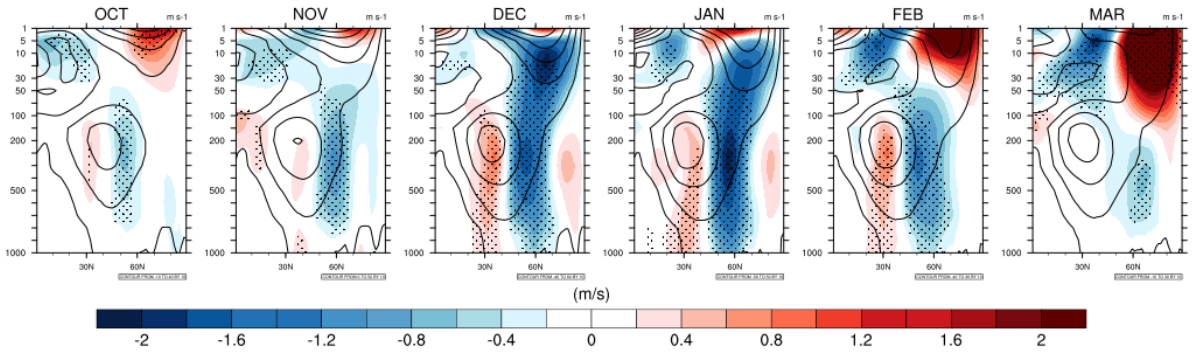

Figure 6: Monthly evolution of the ensemble-mean change in zonal-mean zonal wind between the future-Arctic experiment and the present-day experiment (colours) shown with the present-day climatology (solid black lines) from October to March from CNRM-CM6.

noise ratio could be too small in the models (Scaife and Smith, 2018) such that in reality the response is stronger relative to internal variability.

Future work within APPLICATE will aim to understand the causes of the model diversity, and hence develop an emergent constraint to diagnose the real-world response to Arctic sea-ice loss (Smith et al., 2017).

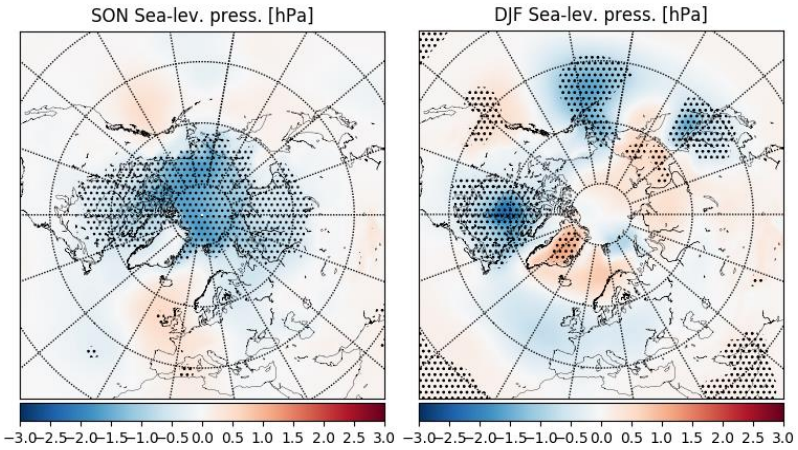

Figure 7: Ensemble-mean change in sea-level pressure between the future-Arctic and the present-day experiment (colours) from EC-Earth. Fields are shown for autumn (SON; left) and winter (DJF; right). Stippling is as in Figure 2. Units are K.

While the focus of the present report is on the Northern Hemisphere, changes are also seen in the Southern Hemisphere (Figures 1, 3, 4, 13, 14, 25, 26, 27). Tropospheric and stratospheric pathways that can potentially explain this cross-hemispheric teleconnection are currently being explored.

3.3 Sea-level pressure

The change in sea-level pressure is most pronounced during autumn and winter when the changes in temperature are strongest (Figure 7 above and Figures 12, 16, 20, 24, and 27 in annex 7.1). During autumn, a significant low-pressure anomaly is found over the central Arctic and over some adjacent land areas, though the exact location of the strongest response varies somewhat between the models. There are also patches of increase in adjacent areas further south, but these are mostly weak and again the locations vary from model to model. The winter response is also model dependant, but common features seem to be patches of significant negative pressure anomalies over the northern Pacific and North-eastern North America, and interestingly a rather consistent increase in sea-level pressure over the Norwegian and Icelandic seas, and a weakening further south. Though the significance varies between the models, a reduction in the pressure gradient between Iceland and the Azores is consistent with a negative phase of the North Atlantic Oscillation (NAO), which is in line with an equatorward shift in the tropospheric jet.

3.4 Changes in extreme events

Changes in tropospheric jets are highly relevant to European weather patterns and extreme events that effect society, including the energy sector supply and demand (e.g. Clark et al, 2017) and transport (e.g. Palin et al, 2016). A recent APPLICATE led energy case study (APPLICATE case study 1) highlights the potential role of low autumn Arctic sea ice leading to extreme climate events at mid-latitudes in the following winter, such as the extremely low precipitation experienced in Europe for winter 2016/2017 alongside unusually low wind speeds. Further evidence for this is provided by the HadGEM3-GA7.1 simulations, which show a significant decrease in winter winds and precipitation over Northern Europe in response to a reduction in Arctic sea ice (Figure 8). Though mostly insignificant here, the drying over the Mediterranean and the wetting seen over central Europe is similar to that seen in response to global warming of 2.0 °C in the multi-model ensemble "HAPPI" (Mitchell et al., 2016) in Li et

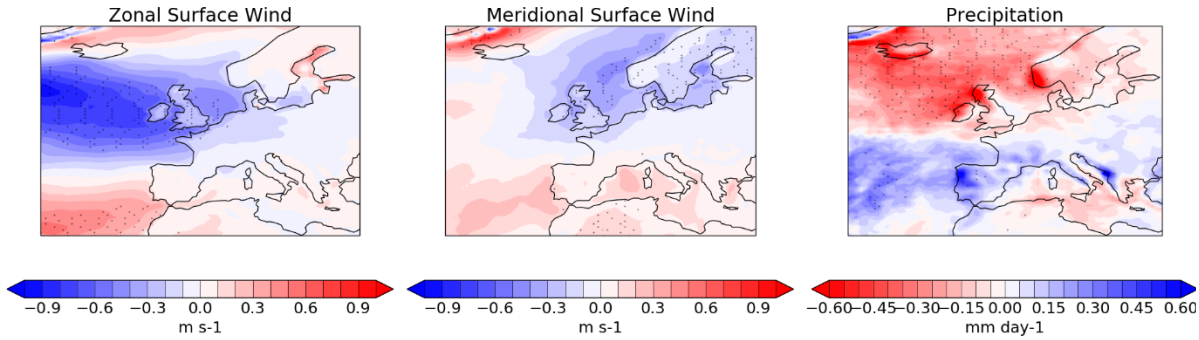

Figure 8: Ensemble-mean change in the zonal surface wind (left), meridional surface wind (middle), and precipitation during winter (DJF; right) from HadGEM3. Units are m s^{-1} (a–b) and mm day^{-1}(c).

al. (2018). The Mediterranean region has also been projected to undergo drying under the forcing of the Representative Concentration Pathway (RCP) scenario corresponding to an increased radiative forcing of 8.5 W m^{-2} by the end of the 21st century (RCP8.5; van Vuuren et al., 2011) in 17 CMIP5 models (Zappa et al., 2015).

Both the causes of and recent changes in mid-latitudes extreme weather have been important topics in recent years. In particular, a lot of attention has been given to the possible links between Arctic amplification, changes in atmospheric flow waviness (amplified Rossby planetary and synoptic waves) and extreme weather. We revisit this topic by characterizing the daily atmospheric flow "waviness" using the waviness index (WAVI; see annex 7.2 for details), a Rossby wave packet based approach, focusing on the regional scales at mid-latitudes and on the 1950-to-present period. We then assess whether there is any evidence supporting long-term changes in monthly waviness between the future-Arctic and the present-day experiments from the CNRM-CM6 model (Voldoire et al., 2019), focusing on both planetary-scale waves (wavenumbers 1–3) and synoptic-scale waves (wavenumbers 4–7). We calculate the waviness index for all days and for 100 members from the future-Arctic and present-day experiments (the full set of members will be analyzed in the near future).

Figure 9 shows the WAVI distributions for synoptic- and planetary-scale waves for summer and winter for the two experiments. The p-values in the plots give the probability of the distributions from the future-Arctic and the present-day climate not being significantly different (the null hypothesis) at a 5% confidence level. Results show that the null hypothesis cannot be robustly rejected for synoptic-scale waves, and in conclusion here is no evidence that the two WAVI distributions simulated by the CNRM-CM6 model are significantly different in winter or summer. This implies that there is no robust and detectable influence of Arctic sea-ice loss on mid-latitudes flow waviness for this specific model and these specific experiments. However, Figure 9 shows that the null hypothesis can be rejected in summer for planetary waves. Inspecting changes for specific quantiles shows that Arctic sea-ice loss has reduced the WAVI median by 1% and increased the 95th percentile by 2%. Mechanisms underlying this potential albeit rather small influence of Arctic sea ice on planetary waves are currently being investigated. Future work will assess if these results hold across all PAMIP models and extend the analysis to a more regional scale (Europe).

The waviness of the flow in the future-Arctic and present-day experiments has also been investigated for the simulations from ECHAM6.3 model using the sinuosity index defined by Cattiaux et al. (2016). The index can be used to judge whether the flow has become less zonal in response to Arctic sea-ice loss. When the sinuosity index is 1, this indicates that the flow is completely zonal, and when values deviate from 1 it indicates that the flow is less zonal and thus varies more meridionally. Note that impacts due to seasonal variations and climate change

are by definition filtered out.

Results show that there is no detectable difference in sinuosity between the future-Arctic and the present-day experiments (comparing the solid brown and red lines in Figure 10). The changes between the two experiments are in fact smaller than the ensemble-spread within each experiment. Considering some of the other PAMIP experiments, the figure shows that when differences between experiments occur, they are mainly associated with changes in SST (compare for instance the solid purple and yellow lines), rather than changes in sea ice.

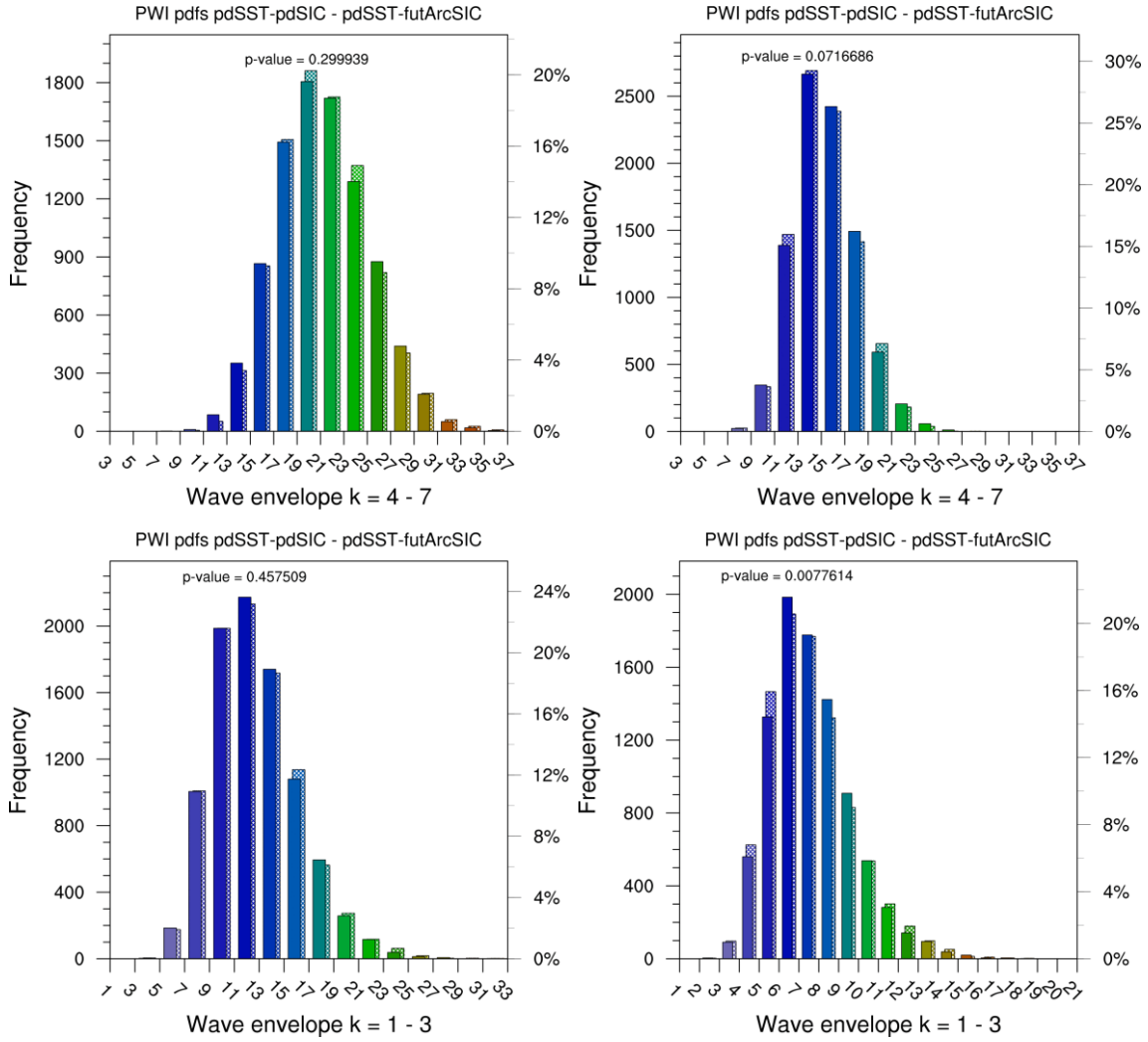

Figure 9: Distributions of synoptic-scale WAVI (top) and planetary-scale WAVI (bottom) for winter (left) and summer (right) for the present-day experiment (full bars) and future-Arctic experiment (hatched bars). The probability of finding the distributions from the future-Arctic and the present-day experiments in the same climate (the p-values) at a 5% confidence level are given in each plot. The p-values were computed using the Kolmogorov-Smirnov two-sample test. The unit on the y-axes is days on the left and percentage on the right. The x-axis gives the WAVI bins in m s^{-1}. Note that the bin range differs between plots to emphasize differences.

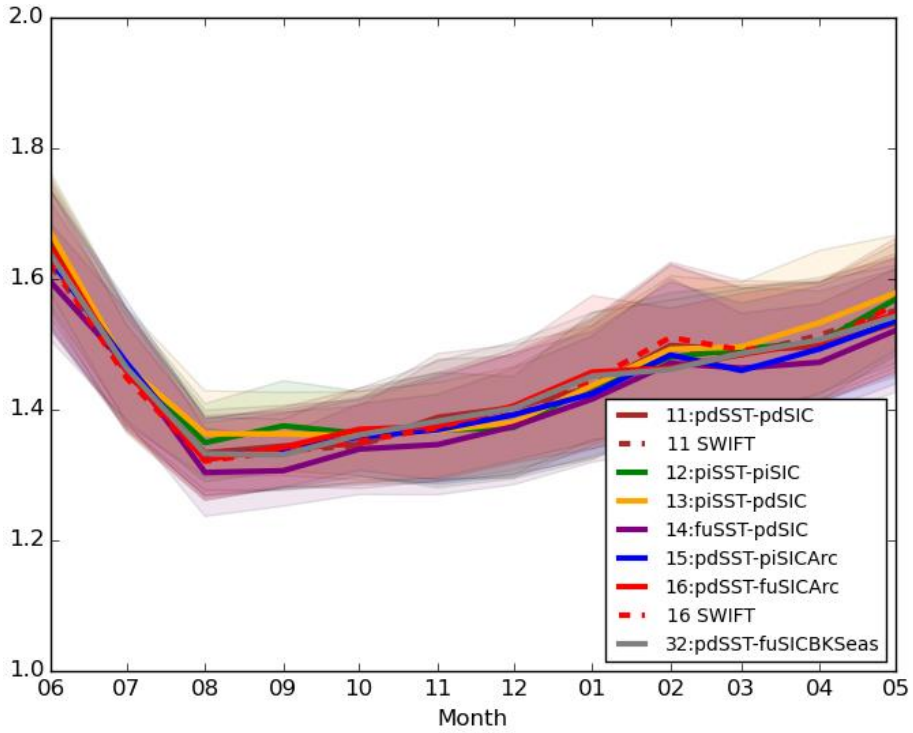

Figure 10: Sinuosity index (Cattiaux et al., 2016) for the present-day experiment (pdSST-pdSIC; solid brown line) and the future-Arctic experiment (pdSST-futArcSIC; solid red line) shown with results from five other PAMIP experiments: the pre-industrial SST and SIC experiment (piSST-piSIC; solid green line), the pre-industrial SSTs and present-day SIC experiment (piSST-pdSIC; solid yellow line), the future SSTs (taken from a future state that is 2 °C warmer than pre-industrial conditions) and present-day SIC experiment (futSST-pdSIC; solid purple line), present-day SSTs and pre-industrial SIC in the Arctic only experiment (pdSST-piSICArc; solid blue line, and the present-day SSTs and future-Arctic SIC only in the Barents Kara Seas experiment (pdSST-fuSICBKSeas; solid grey line). The dashed lines represent experiments where the ozone chemistry in the polar stratosphere has been switched on (SWIFT module from AWI Potsdam).

4. CONCLUSIONS AND OUTLOOK

In this report, we have we investigated the effect of Arctic sea-ice decline by examining results from two experiments in which the sea ice is either prescribed to values corresponding to the present-day climate or a future climate with reduced sea ice in the Arctic. The experiments have been carried out by APPLICATE partners with a number of state-of-the-art climate models (Table 1).

Results show that sea-ice loss in the Arctic is associated with significant low-level warming over the Arctic region. The warming is strongest during boreal autumn and winter, when the changes in sea ice between the future-Arctic and the present-day experiments are most pronounced. The change in near-surface temperature is largest over the Arctic Basin during autumn and more over the marginal seas during winter.

Changes in near-surface temperature are also found over land. There is significant warming in regions in Eastern Europe, Siberia, and North America (consistent with Peings et al., 2014). However, the extent and magnitude of the warming seems to be model dependent.

We find a robust weakening of the tropospheric winter jet on the poleward side of the climatological maximum in the models. For the majority of the models, there is also an intensification on the equatorward side. There is, however, large variation in the magnitude and even sign of the response of the stratospheric jet. The latter is shown to exhibit substantial seasonal variability in CNRM-CM6, a behaviour which complicates the interpretation of seasonal means and comparison between models and warrants looking at monthly evolution of the changes in zonal-mean zonal wind when investigating the stratospheric response.

The change in sea-level pressure is also largest in the cold seasons. We find a significant low-pressure anomaly residing over the central Arctic during fall. During winter, the response varies more from model to model, but there is a rather consistent increase in the Icelandic region and decrease further south, in line with a negative phase of the NAO and an equatorward shift of the tropospheric jet.

Changes in tropospheric jets have potential ramifications for European weather patterns and extreme events that effect society. A recent APPLICATE led energy case study (APPLICATE case study 1) highlights the potential role of low autumn Arctic sea ice leading to extreme climate events at mid-latitudes in the following winter. Further evidence for this is seen in the HadGEM3-GA7.1 simulations, which show a significant decrease in winter winds and precipitation over Northern Europe in response to a reduction in Arctic sea ice (Figure 8).

Changes in weather extremes and Arctic amplification have recently been linked to changes in the waviness of the atmospheric flow. Using the waviness index WAVI, we find a significant influence of Arctic sea-ice loss on planetary-scale waves during summer in CNRM-CM6. However, significant differences are not found for planetary-scale waves during winter, nor for synoptic-scale waves during summer or winter. These results are corroborated by an analysis for ECHAM6.3, using the sinuosity index proposed by Cattiaux et al. (2016), which shows that differences in sinuosity between the future-Arctic and the present-day experiments are rather small. Furthermore, this analysis shows that changes in SSTs are more influential on the sinuosity index than changes in sea ice.

Results from the experiments examined here and from other experiments defined under the PAMIP protocol will continue to be analysed within the APPLICATE and the PAMIP community. Key goals are to understand the physical processes, and to take advantage of the multi-model spread, to diagnose the real-world situation. There are several on-going projects, including projects on the refractive index constraint on jet response (Doug Smith, Elisa Manzini, Michael Sigmond), summer extremes (Laurent Terray), waviness and blocking (Tido Semmler, Russell Blackport, Gudrun Magnusdottir), Siberian/Eurasian cooling (James Screen/Russell Blackport, Gudrun Magnusdottir, Masato Mori), the poleward heat transport response to sea ice and SST (Paul Kushner, Yutian Wu), interhemispheric connections (Rosie Eade, Xavier Levine), stratosphere-troposphere coupling (Yannick Peings, Jinro Ukita, Jiankai Zhang), the Antarctic response (Holly Ayres), the sensitivity to background state/nonlinearity (Rym Msadek), dynamical versus thermodynamical responses (Rym Msadek), the quasi-biennial oscillation and response to sea-ice anomalies (Guillaume Gastineau), and the causality links behind the sea ice and atmosphere links in observations and models (Guillaume Gastineau).

5. REFERENCES

APPLICATE case study 1: Energy case study. Effects of Arctic sea ice on energy production in mid-latitudes, https://applicate.eu/images/news/2019/Energy_case_study_APPLICATE_V3.pdf.

Blackport, R. and Kushner, P. J.: The Transient and Equilibrium Climate Response to Rapid Summertime Sea Ice Loss in CCSM4, Journal of Climate, 29, 401–417, https://doi.org/10.1175/JCLI-D-15-0284.1, 2016.

Blackport, R. and Kushner, P. J.: Isolating the Atmospheric Circulation Response to Arctic Sea Ice Loss in the Coupled Climate System, Journal of Climate, 30, 2163–2185, https://doi.org/10.1175/JCLI-D-16-0257.1, 2017.

Cattiaux, J., Peings, Y., Saint-Martin, D., Trou-Kechout, N., and Vavrus, S. J.: Sinuosity of midlatitude atmospheric flow in a warming world, Geophysical Research Letters, 43, 8259–8268, https://doi.org/10.1002/2016GL070309, 2016.

Clark, R. T., Bett, P. E., Thornton, H. E., and Scaife, A. A.: Skilful seasonal predictions for the European energy industry, Environmental Research Letters, 12, 024 002, https://doi.org/10.1088/1748-9326/aa57ab, 2017.

Deser, C., Tomas, R. A., and Sun, L.: The Role of Ocean–Atmosphere Coupling in the Zonal-Mean Atmospheric Response to Arctic Sea Ice Loss, Journal of Climate, 28, 2168–2186, https://doi.org/10.1175/JCLI-D-14-00325.1, 2015.

Fragkoulidis, G., Wirth, V., Bossmann, P., and Fink, A. H.: Linking Northern Hemisphere temperature extremes to Rossby wave packets, Quarterly Journal of the Royal Meteorological Society, 144, 553–566, https://doi.org/10.1002/qj.3228, 2018.

Honda, M., Inoue, J., and Yamane, S.: Influence of low Arctic sea-ice minima on anomalously cold Eurasian winters, Geophysical Research Letters, 36, https://doi.org/10.1029/2008GL037079, 2009.

Irving, D. and Simmonds, I.: A Novel Approach to Diagnosing Southern Hemisphere Planetary Wave Activity and Its Influence on Regional Climate Variability, Journal of Climate, 28, 9041–9057, https://doi.org/10.1175/JCLI-D-15-0287.1, 2015.

Li, C., Michel, C., Seland Graff, L., Bethke, I., Zappa, G., Bracegirdle, T. J., Fischer, E., Harvey, B. J., Iversen, T., King, M. P., Krishnan, H., Lierhammer, L., Mitchell, D., Scinocca, J., Shiogama, H., Stone, D. A., and Wettstein, J. J.: Midlatitude atmospheric circulation responses under 1.5 and 2.0 ◦ C warming and implications for regional impacts, Earth System Dynamics, 9, 359–382, https://doi.org/10.5194/esd-9-359-2018, https://www.earth-syst-dynam.net/9/359/2018/, 2018.

Mori, M., Watanabe, M., Shiogama, H., Inoue, J., and Kimoto, M.: Robust Arctic sea-ice influence on the frequent Eurasian cold winters in past decades, Nature Geoscience, 7, 869–873, https://doi.org/10.1038/ngeo2277, 2014.

Mori, M., Kosaka, Y., Watanabe, M., Nakamura, H., and Kimoto, M.: A reconciled estimate of the influence of Arctic sea-ice loss on recent Eurasian cooling, Nature Climate Change, 9, 139–129, https://doi.org/10.1038/s41558-018-0379-3, 2019.

Oudar, T., Sanchez-Gomez, E., Chauvin, F., Cattiaux, J., Terray, L., and Cassou, C.: Respective

roles of direct GHG radiative forcing and induced Arctic sea ice loss on the Northern Hemisphere atmospheric circulation, Climate Dynamics, 49, 3693–3713, https://doi.org/10.1007/s00382-017-3541-0, 2017.

Palin, E. J., Scaife, A. A., Wallace, E., Pope, E. C. D., Arribas, A., and Brookshaw, A.: Skillful Seasonal Forecasts of Winter Disruption to the U.K. Transport System, Journal of Applied Meteorology and Climatology, 55, 325–344, https://doi.org/10.1175/JAMC-D-15-0102.1, 2016.

Peings, Y. and Magnusdottir, G.: Response of the Wintertime Northern Hemisphere Atmospheric Circulation to Current and Projected Arctic Sea Ice Decline: A Numerical Study with CAM5, Journal of Climate, 27, 244–264, https://doi.org/10.1175/JCLI-D-13-00272.1, 2014.

Röthlisberger, M., Pfahl, S., and Martius, O.: Regional-scale jet waviness modulates the occurrence of midlatitude weather extremes, Geophysical Research Letters, 43, 10,989–10,997, https://doi.org/10.1002/2016GL070944, 2016.

Scaife, A. A. and Smith, D.: A signal-to-noise paradox in climate science, npj Climate and Atmospheric Science, 1, https://doi.org/10.1038/s41612-018-0038-4, 2018.

Screen, J. A., Deser, C., Smith, D. M., Zhang, X., Blackport, R., Kushner, P. J., Oudar, T. A., McCusker, K. E., and Sun, L.: Consistency and discrepancy in the atmospheric response to Arctic sea-ice loss across climate models, Nature Geoscience, pp. 155–163, https://doi.org/10.1038/s41561-018-0059-y, 2018.

Smith, D. M., Dunstone, N. J., Scaife, A. A., Fiedler, E. K., Copsey, D., and Hardiman, S. C.: Atmospheric Response to Arctic and Antarctic Sea Ice: The Importance of Ocean–Atmosphere Coupling and the Background State, Journal of Climate, 30, 4547–4565, https://doi.org/10.1175/JCLI-D-16-0564.1, 2017.

Smith, D. M., Screen, J. A., Deser, C., Cohen, J., Fyfe, J. C., García-Serrano, J., Jung, T., Kattsov, V., Matei, D., Msadek, R., Peings, Y., Sigmond, M., Ukita, J., Yoon, J.-H., and Zhang, X.: The Polar Amplification Model Intercomparison Project (PAMIP) contribution to CMIP6: investigating the causes and consequences of polar amplification, Geoscientific Model Development, 12, 1139–1164, https://doi.org/10.5194/gmd-12-1139-2019, 2019.

van Vuuren, D. P., Edmonds, J., Kainuma, M., Riahi, K., Thomson, A., Hibbard, K., Hurtt, G. C., Kram, T., Krey, V., Lamarque, J.-F., Masui, T., Meinshausen, M., Nakicenovic, N., Smith, S. J., and Rose, S. K.: The representative concentration pathways: an overview, Climatic Change, 109, 5, https://doi.org/10.1007/s10584-011-0148-z, 2011.

Voldoire, A., Saint-Martin, D., Sénési, S., Decharme, B., Alias, A., Chevallier, M., Colin, J., Guérémy, J.-F., Michou, M., Moine, M.-P., Nabat, P., Roehrig, R., Salas y Mélia, D., Séférian, R., Valcke, S., Beau, I., Belamari, S., Berthet, S., Cassou, C., Cattiaux, J., Deshayes, J., Douville, H., Ethé, C., Franchistéguy, L., Geoffroy, O., Lévy, C., Madec, G., Meurdesoif, Y., Msadek, R., Ribes, A., Sanchez-Gomez, E., Terray, L., and Waldman, R.: Evaluation of CMIP6 DECK Experiments With CNRM-CM6-1, Journal of Advances in Modeling Earth Systems, 11, 2177–2213, https://doi.org/10.1029/2019MS001683, 2019.

Wilks, D. S.: "The Stippling Shows Statistically Significant Grid Points": How Research Results are Routinely Overstated and Overinterpreted, and What to Do about It, Bulletin of the American Meteorological Society, 97, 2263–2273, https://doi.org/10.1175/BAMS-D-15-00267.1, 2016.

Wirth, V., Riemer, M., Chang, E. K. M., and Martius, O.: Rossby Wave Packets on the Midlatitude Waveguide—A Review, Monthly Weather Review, 146, 1965–2001, https://doi.org/10.1175/MWR-D-16-0483.1, 2018.

Zappa, G., Hawcroft, M. K., Shaffrey, L., Black, E., and Brayshaw, D. J.: Extratropical cyclones and the projected decline of winter Mediterranean precipitation in the CMIP5 models, Climate Dynamics, 45, 1727–1738, https://doi.org/10.1007/s00382-014-2426-8, 2015.

Zimin, A. V., Szunyogh, I., Patil, D. J., Hunt, B. R., and Ott, E.: Extracting Envelopes of Rossby Wave Packets, Monthly Weather Review, 131, 1011–1017, https://doi.org/10.1175/1520-0493(2003)131<1011:EEORWP>2.0.CO;2, 2003.

6. ACRONYMS

DJF: December, January, and February

JJA: June, July, and August

MAM: March, April, and May

NAO: North Atlantic Oscillation

SON: September, October, and November

SIC: Sea Ice Concentration

SST: Sea Surface Temperature

WAVI: Wave Activity Index

7. ANNEXES

7.1 The individual model responses

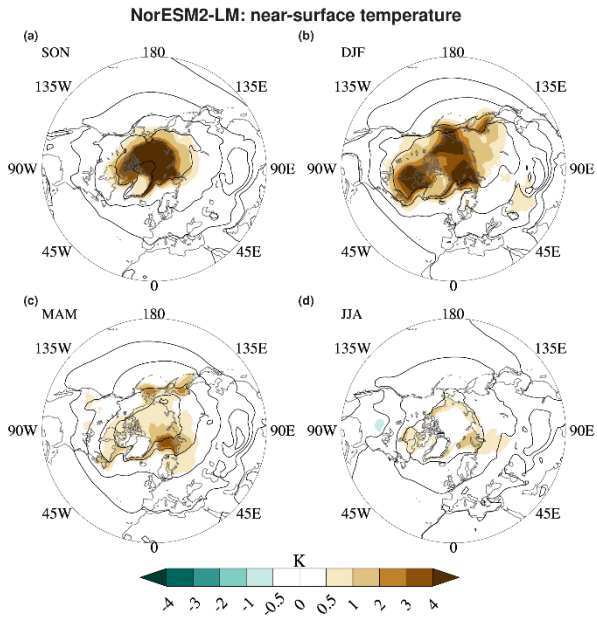

*Figure 11: Ensemble-mean change in near-surface temperature between the future-Arctic and the present-day experiment (colours) shown with the present-day climatology (solid black contours) for NorESM2-LM. Fields are shown for SON (a), DJF (b), MAM (c), and JJA (d). White dots indicate that the results are **not significant** at the 5% level by the Welch t-test. Units are K.*

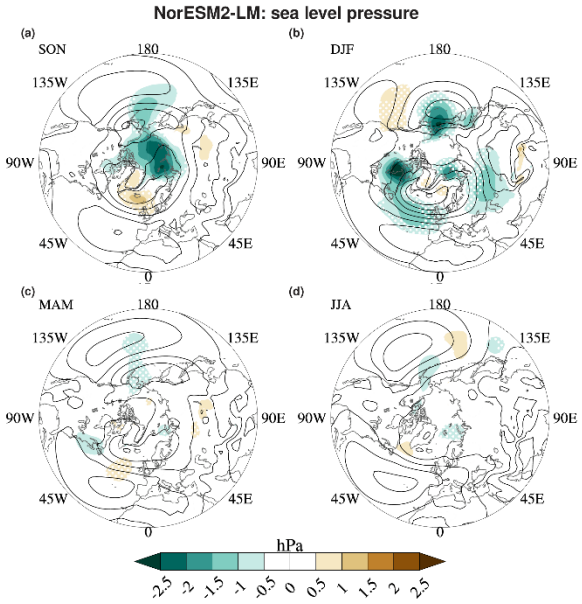

Figure 12: As in Figure 11, but for sea-level pressure. Units are hPa.

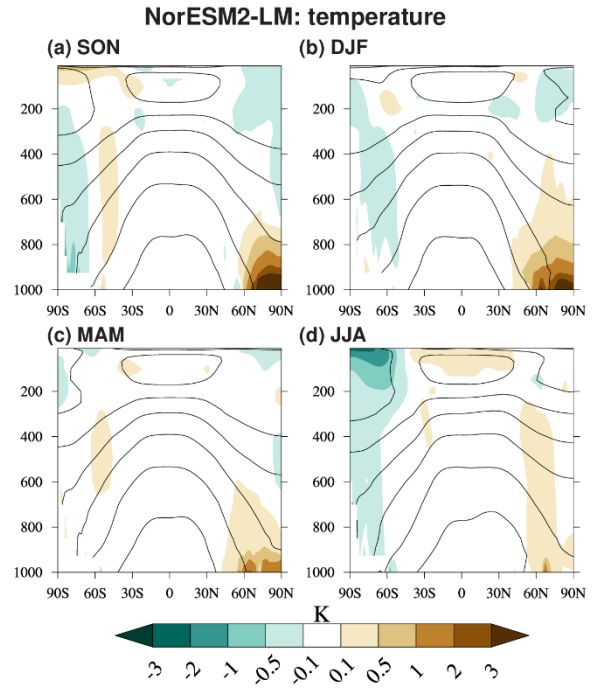

Figure 13: As in Figure 11, but for zonal-mean temperature. Units are K.

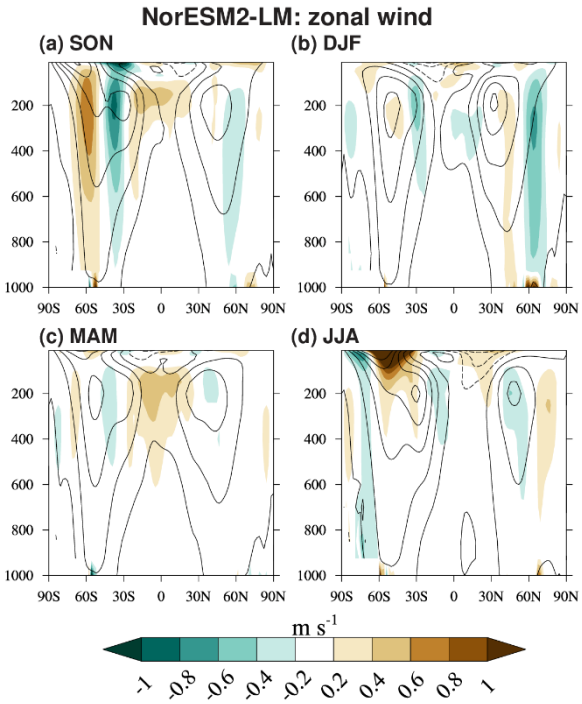

Figure 14: As in Figure 11, but for zonal-mean zonal wind. Units are m s^{-1}.

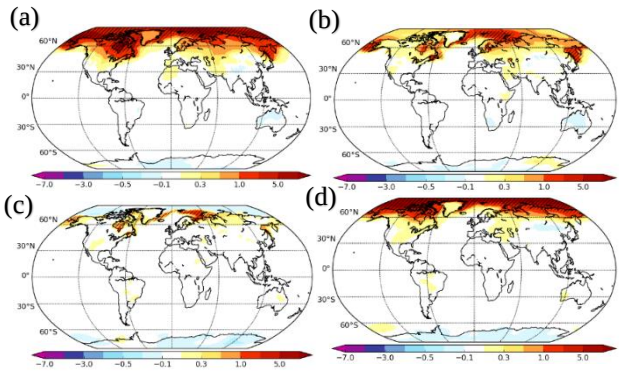

Figure 15: Ensemble-mean multi-model-mean change in near-surface temperature between the future-Arctic and the present-day experiment (colours) for ECHAM6.3/OpenIFS. Results are shown for DJF (a), MAM (b), JJA (c), and SON (d). Shading indicates that the results are significant. Units are ºC.

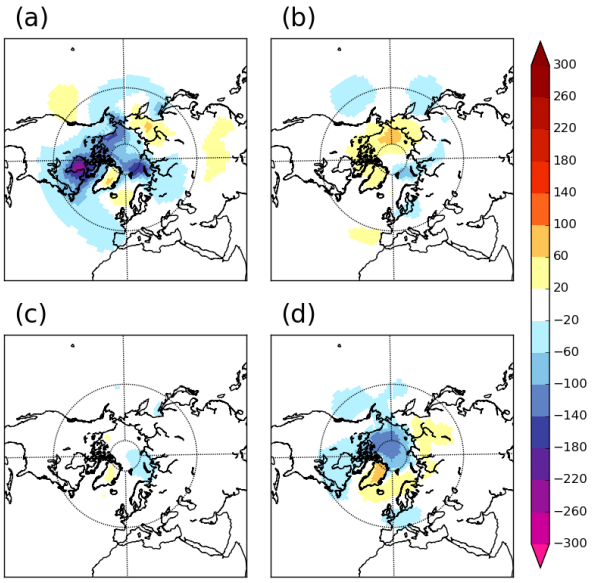

Figure 16: As in Figure 15, but for sea-level pressure. Units are Pa.

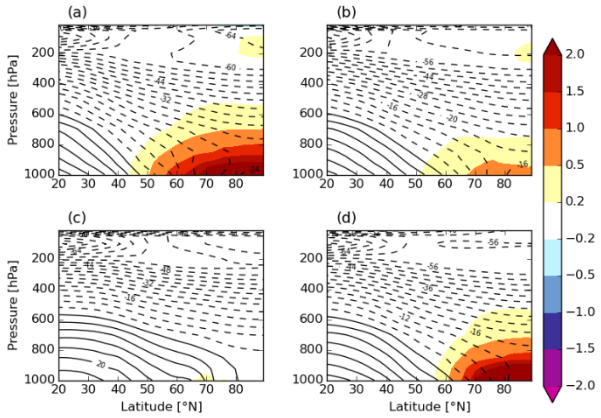

Figure 17: As in Figure 15, but for zonal-mean temperature (colours) shown with the present-day climatology (solid black lines for positive values and dashed black lines for negative values). Units are °C.

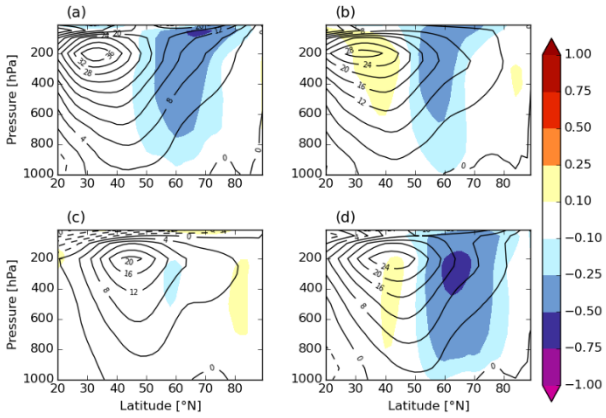

Figure 18: As in Figure 15, but for the zonal-mean zonal wind (colours) shown with the present-day climatology (solid black lines). Units are m s^{-1}.

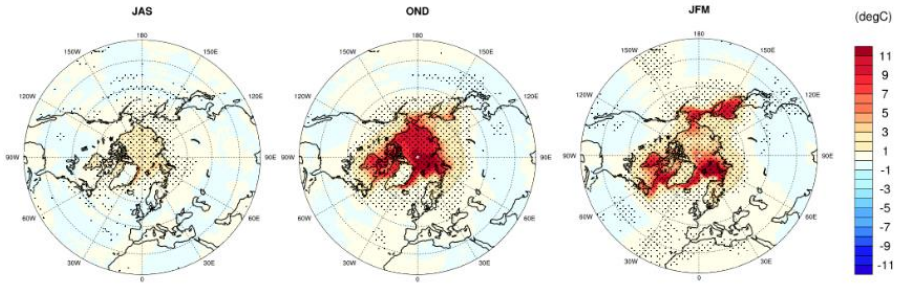

Figure 19: Ensemble-mean change in near-surface temperature between the future-Arctic and the present-day experiment (colours) from CNRM-CN6. The results are shown for summer, here defined as the three-month period June–September (JAS; left), autumn, defined as October–December (OND; middle), and winter, defined as January–March (JFM; right). Note that the seasons are defined slightly differently here compared to figures from other models, which may affect the interpretation of the results when comparing between different models. Black dots indicate that differences are significant at the 95% level by the False Discovery Rate (Wilks, 2016). Units are °C.

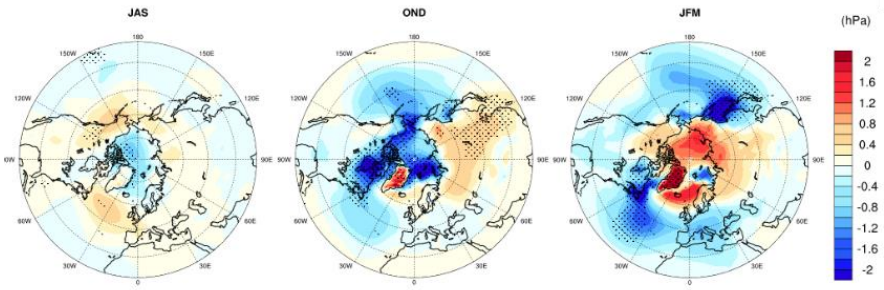

Figure 20: As in Figure 19, but for sea-level pressure. Units are hPa.

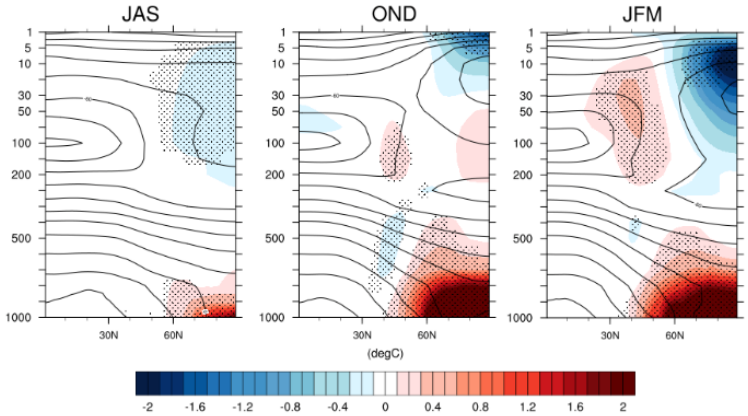

Figure 21: As in Figure 19, but for zonal-mean temperature (colours) shown with the present-day climatology (black solid lines). Units are ºC.

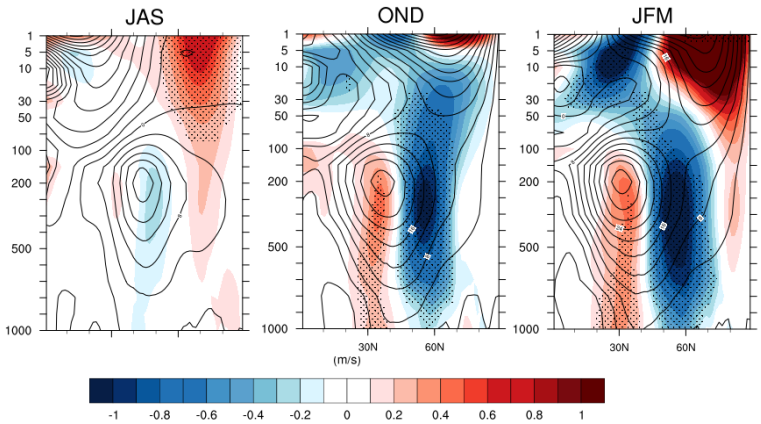

Figure 22: As in Figure 19, but for the zonal-mean zonal wind (colours) shown with the present-day climatology (solid black lines). Units are m s^{-1}.

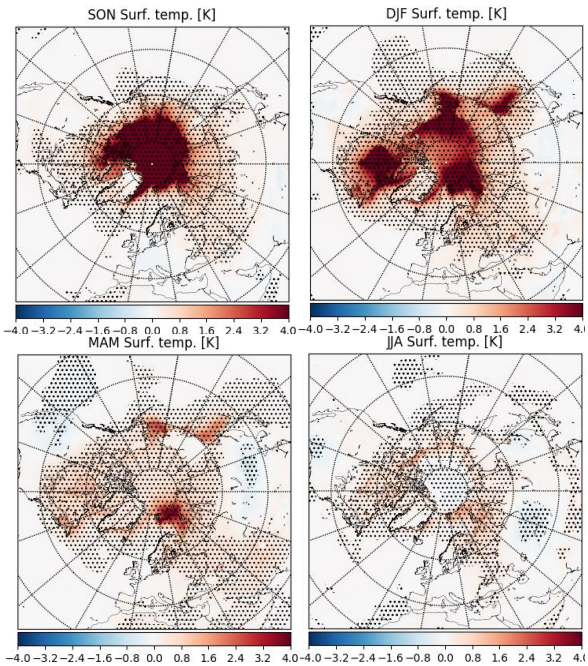

Figure 23: Ensemble-mean change in near-surface temperature between the future-Arctic and the present-day experiment (colours) for EC-Earth. Fields are shown for autumn (SON, upper left), winter (DJF; upper right), spring (MAM; bottom left), and summer (JJA; bottom right). Stippling indicates that the changes are significant at the 95% confidence level. The significance is assessed by computing 1000 samples of ensemble-mean anomalies by randomly bootstrapping members of the present-day and future-Arctic experiments, and requiring for the ensemble-mean anomalies to have the same sign in at least 95% of the bootstrapped samples. Units are K.

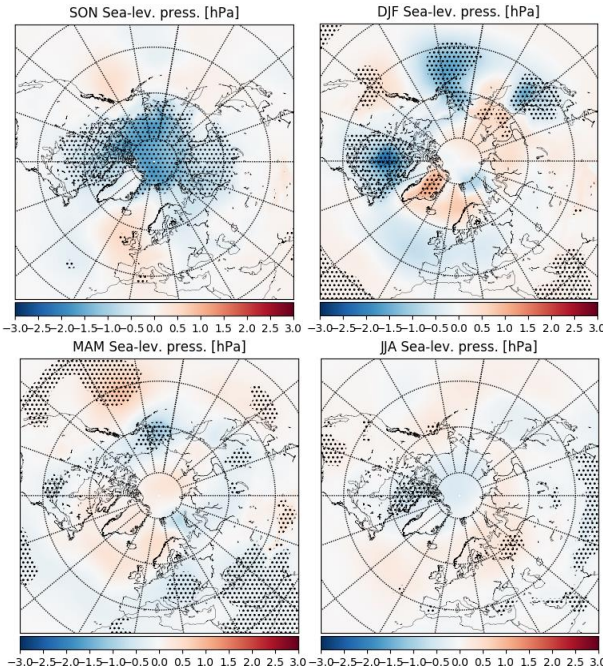

Figure 24: As in Figure 23, but for the change in sea-level pressure. Units are hPa.

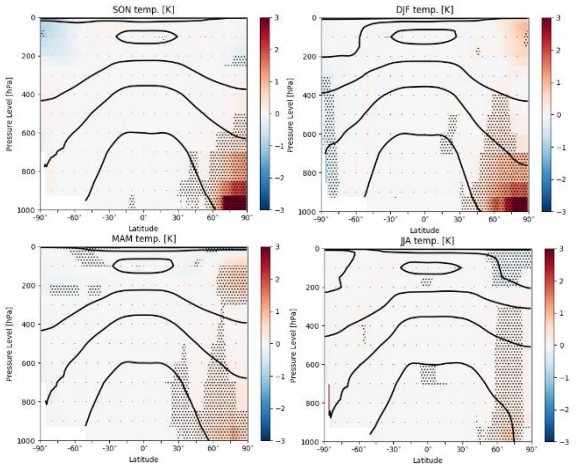

Figure 25: As in Figure 23, but for the change in zonal-mean temperature (colours) shown with the present-day climatology (solid black lines with intervals of 10 K). Units are K.

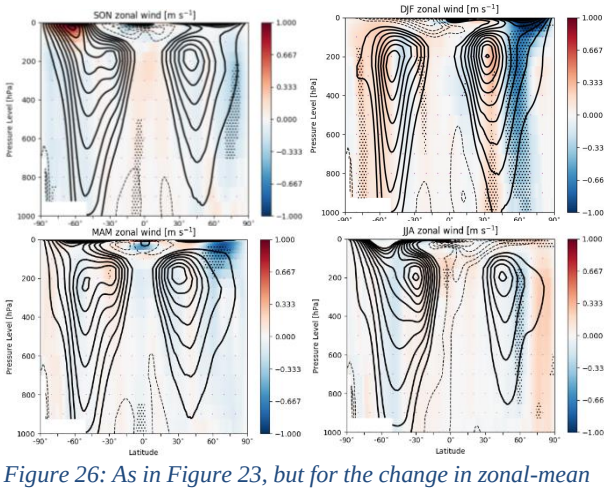

Figure 26: As in Figure 23, but for the change in zonal-mean zonal wind (colours) shown with the present-day climatology (solid black lines with intervals of 4 m s^{-1}). Units are m s^{-1}.

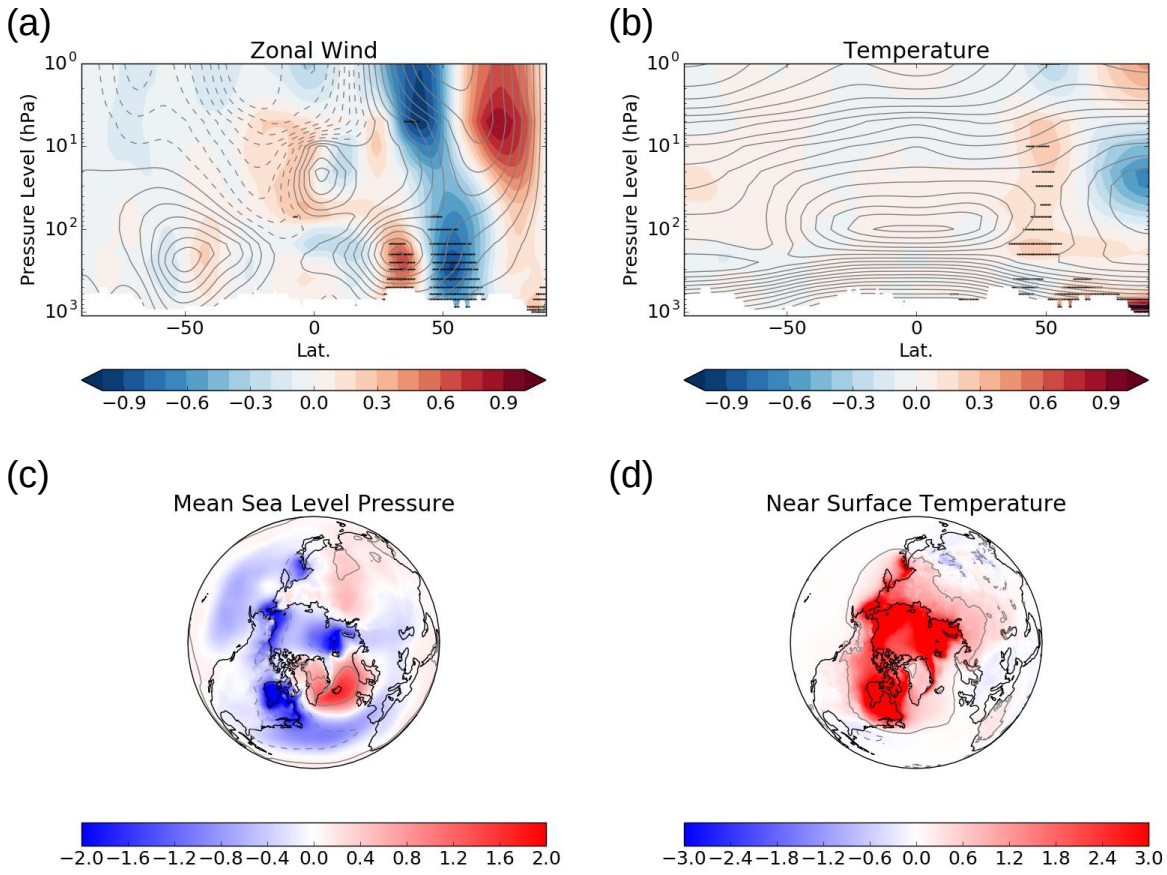

Figure 27: Ensemble-mean change (colours) in zonal-mean zonal wind (a), zonal-mean temperature (b), sea level pressure (c), and near-surface temperature (d) during winter (DJF) from HadGEM3. In a and b, the grey contour lines show the present-day climatology at 5 m s^{-1} and 5 K intervals, with dashed lines representing negative values. Differences that are significant at the 95% level by a student t-test based on ensemble means and variances across the 150 members are marked by stippling (a–b) or highlighting by grey contours (c–d). Units are m s^{-1} (a), K (b, d), and hPa (c).

7.2 The WAVI waviness index

To investigate changes in waviness, we apply the concept of the Rossby wave packet (RWP) to track changes in waviness in the mid-latitudes. RWPs are defined as Rossby waves for which the amplitude has a local maximum and decays to smaller values at larger distances. They are known to act as long-range precursors to extreme weather and be a source of predictability of mid-latitudes weather (Fragkoulidis et al, 2018; Föthlisberger et al., 2016; Wirth et al., 2018). We use a simple waviness index (WAVI) based on RWP amplitude to assess potential changes in atmospheric circulation waviness due to sea-ice loss in the Arctic. The WAVI is based on the RWP envelope reconstruction pioneered by Zimin et al. (2003). The envelope reconstruction involves a Hilbert transform along circles of constant latitude (a sequence of a Fourier transform followed by an inverse Fourier transform) and can be combined with a restriction of the zonal wave numbers to a pre-defined range. We perform the envelope reconstruction for three wave number ranges: k = 1–9 (all waves), k = 1–3 (planetary waves) and k = 4–7 (synoptic waves). The complex number amplitude of the Hilbert transform outcome represents the RWP envelope. The RWP envelope is a three-dimensional field (time, latitude, longitude). Following (Irving and Simmonds, 2015), we transform it to an index which is time-dependent only (i.e., the WAVI) by: (1) calculating the meridional maximum over the range 30°N–65°N, and (2) taking the zonal median to remove the longitudinal dimension. The previous steps are performed for the full hemisphere (they will also be used in a later study for specific regions such as Europe). We use the 300-hPa meridional wind as our wave-like variable because the meridional wind is directly involved with meridional exchanges of heat and moisture which are known to often play a key role in extreme weather events. Sensitivity tests with lower vertical levels give essentially the same results showing the quasi-barotropic character of these waves.